SUPPLEMENTARY DATA

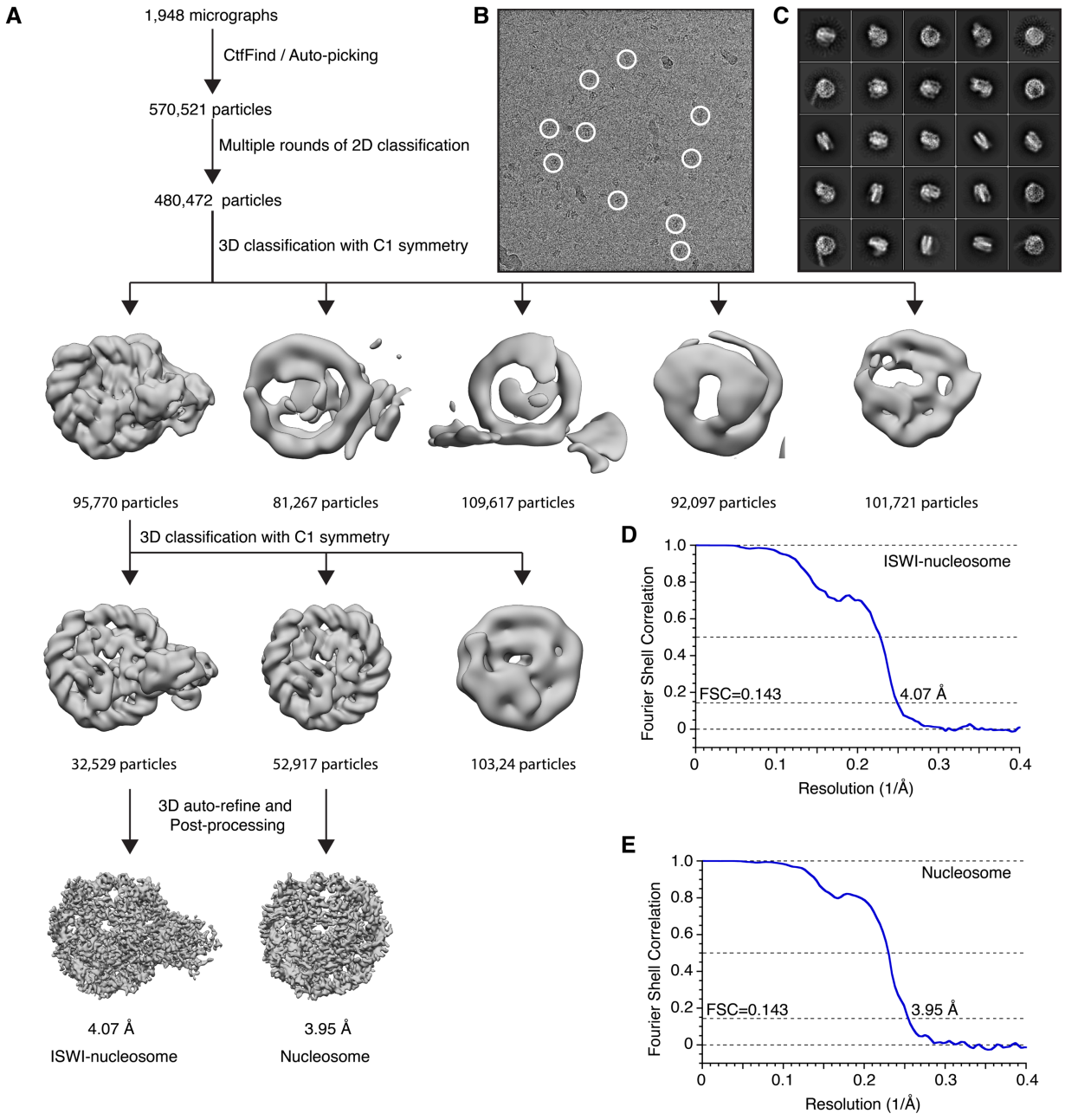

Figure S1. Cryo-EM analysis of the ISWI-nucleosome complex. (A) Overall cryo-EM image processing resulting in the final density maps of the CtISWI$_{77\text{-}\Delta\text{-}722}$-nucleosome complex and free nucleosome. (B) Representative cryo-EM image of CtISWI$_{77\text{-}\Delta\text{-}722}$-nucleosome preparation with

examples of particles highlighted using white circles. (C) Representative 2D class averages. (D and E) Fourier-Shell-Correlation (FSC) curves corresponding to the CtISWI$_{77\text{-}\Delta\text{-}722}$-nucleosome complex (D) and the free nucleosome (E) structures.

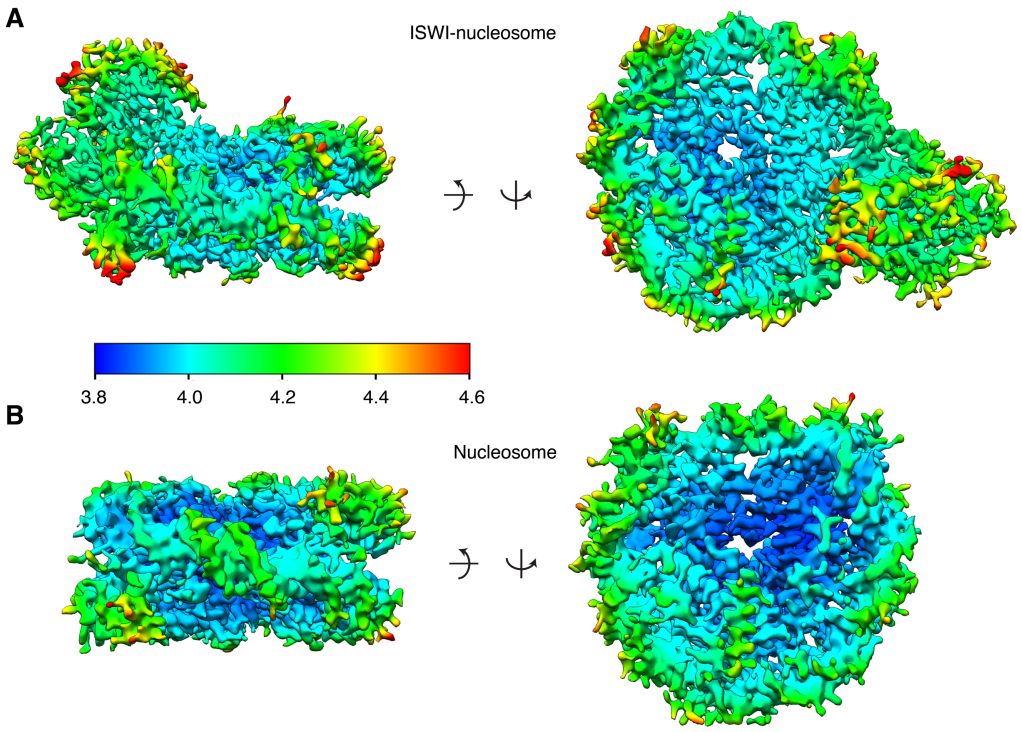

Figure S2. Assessments of the local resolution distribution. (A and B) Two different views of the CtISWI$_{77\text{-}\Delta\text{-}722}$-nucleosome complex (A) and the free nucleosome (B) maps colored using the local resolution as calculated using the Local Resolution module within RELION. The resolution scale bar corresponds to both the panels.

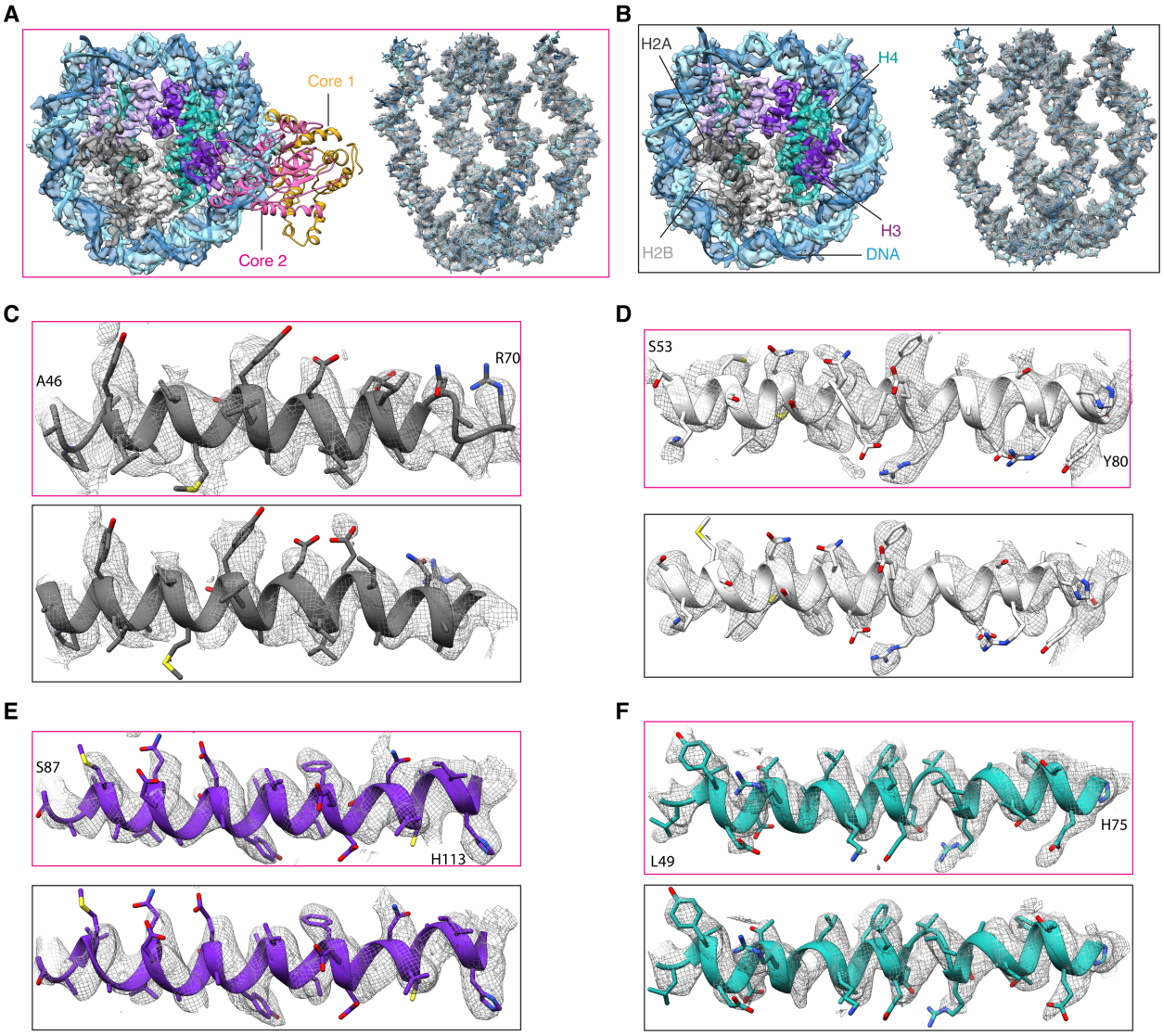

Figure S3. Quality of the map and model building of the nucleosome core. (A) Cryo-EM map of only the nucleosome core particle corresponding to the CtISWI$_{77\text{-}\Delta\text{-}722}$-nucleosome complex fitted with the refined structural model (left panel). A ribbon representation corresponding to the bound CtISWI$_{77\text{-}\Delta\text{-}722}$ is shown to indicate location of the remodeler binding but the density corresponding to remodeler is omitted for clarity. Coloring is same as in Figure 1. In the right panel, extracted density corresponding to the nucleosomal DNA and the fitted model is shown. (B) Same as in panel (A) but for the structure of free nucleosome. (C – F) Density and the fitted

model corresponding to representative segments of histone proteins H2A (C), H2B (D), H3 (E), and H4 (F). The two subpanels show same segment corresponding to the CtISWI$_{77\text{-}\Delta\text{-}722}$-nucleosome complex (top panels) and the free nucleosome (bottom panels). Residue numbering pertaining to each segment is included in the top panels.

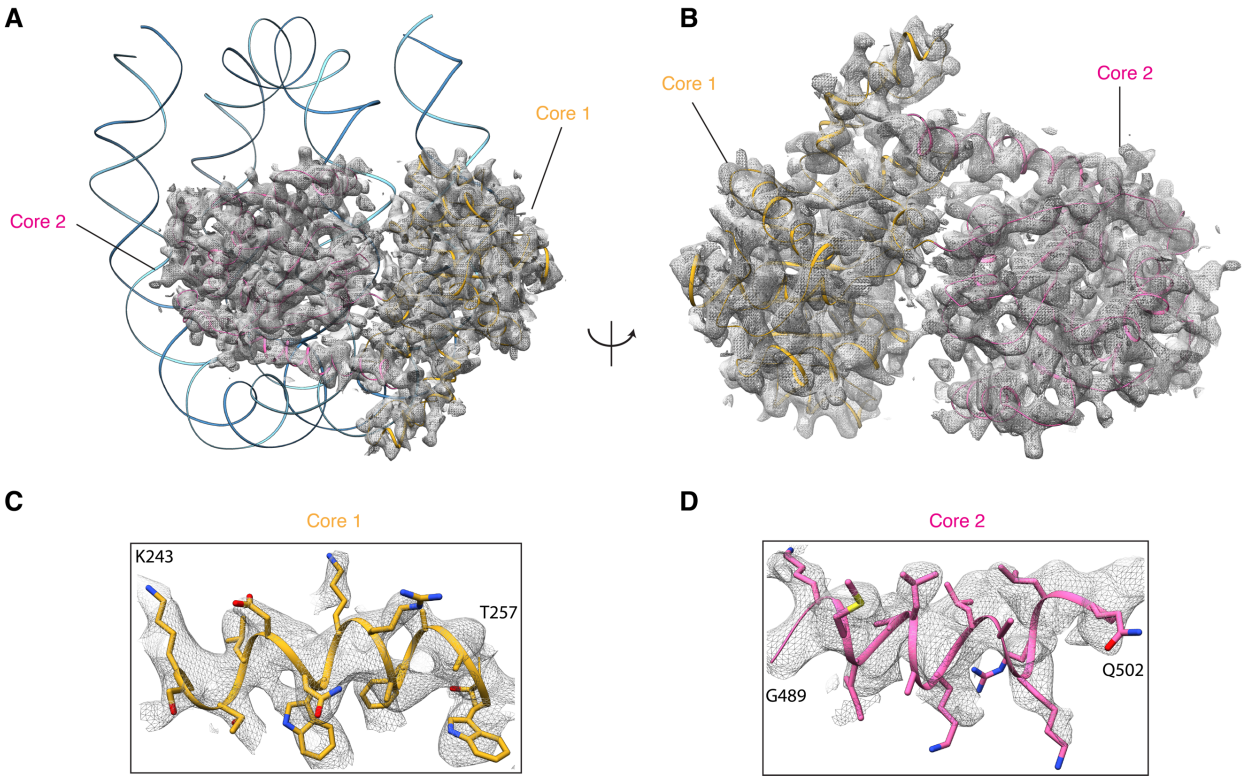

Figure S4. Quality of the map and model building of the nucleosome bound ISWI. (A) A view of the CtISWI$_{77\text{-}\Delta\text{-}722}$ remodeler bound to nucleosome. Histone proteins are omitted for clarity. (b) Close up and rotated view of the panel (A). (C and D) Representative segments from core 1 (C) and core 2 (D) of the ISWI ATPase domain. Residue numbering pertaining to each segment is shown in respective panels.

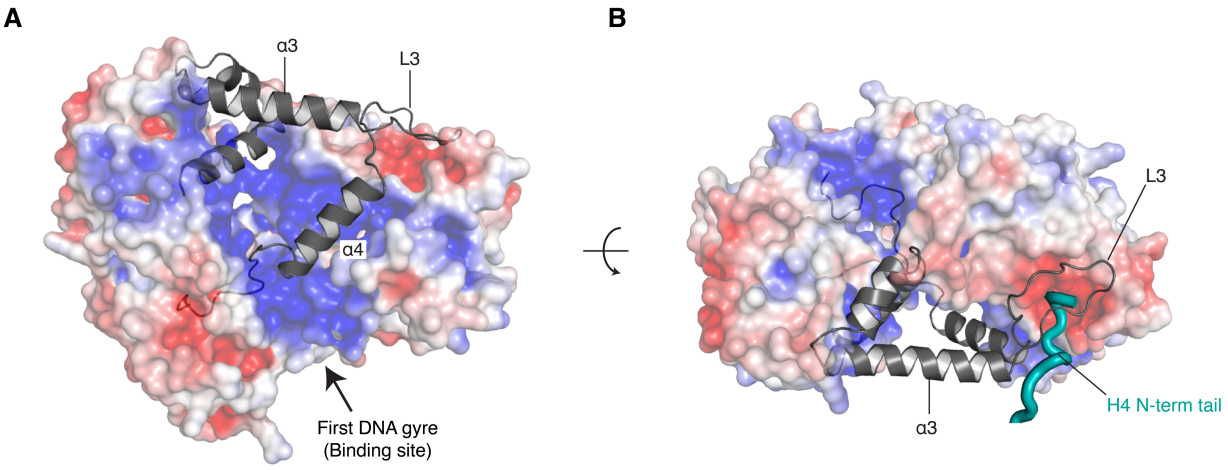

Figure S5. Destabilization of the AutoN domain upon nucleosome binding. **(A)** The AutoN domain from the nucleosome free state of $MtISWI_{81\text{-}723}$ (ribbon shown in black, PDB 5JXR) is docked onto the nucleosome bound state of $CtISWI_{77\text{-}\Delta\text{-}722}$ (shown in surface colored using electrostatic potential – blue: positive, red: negative) using coordinates of the core 2 as the reference. First gyre of the nucleosomal DNA, that occupies the central positively charged cleft in the nucleosome bound state of $CtISWI_{77\text{-}\Delta\text{-}722,}$ and regions beyond the AutoN domain of $MtISWI_{81\text{-}723}$ are omitted for clarity. **(B)** A rotated view to that of the panel (A) but with the addition of the N-terminal tail of histone H4 (teal) as in the nucleosome bound state of $CtISWI_{77\text{-}\Delta\text{-}722}$ that occupies the same acidic patch of ISWI as the L3 loop of AutoN in the nucleosome free state of $MtISWI_{81\text{-}723}$ and the H4 tail in the nucleosome bound state of $CtISWI_{77\text{-}\Delta\text{-}722}$.

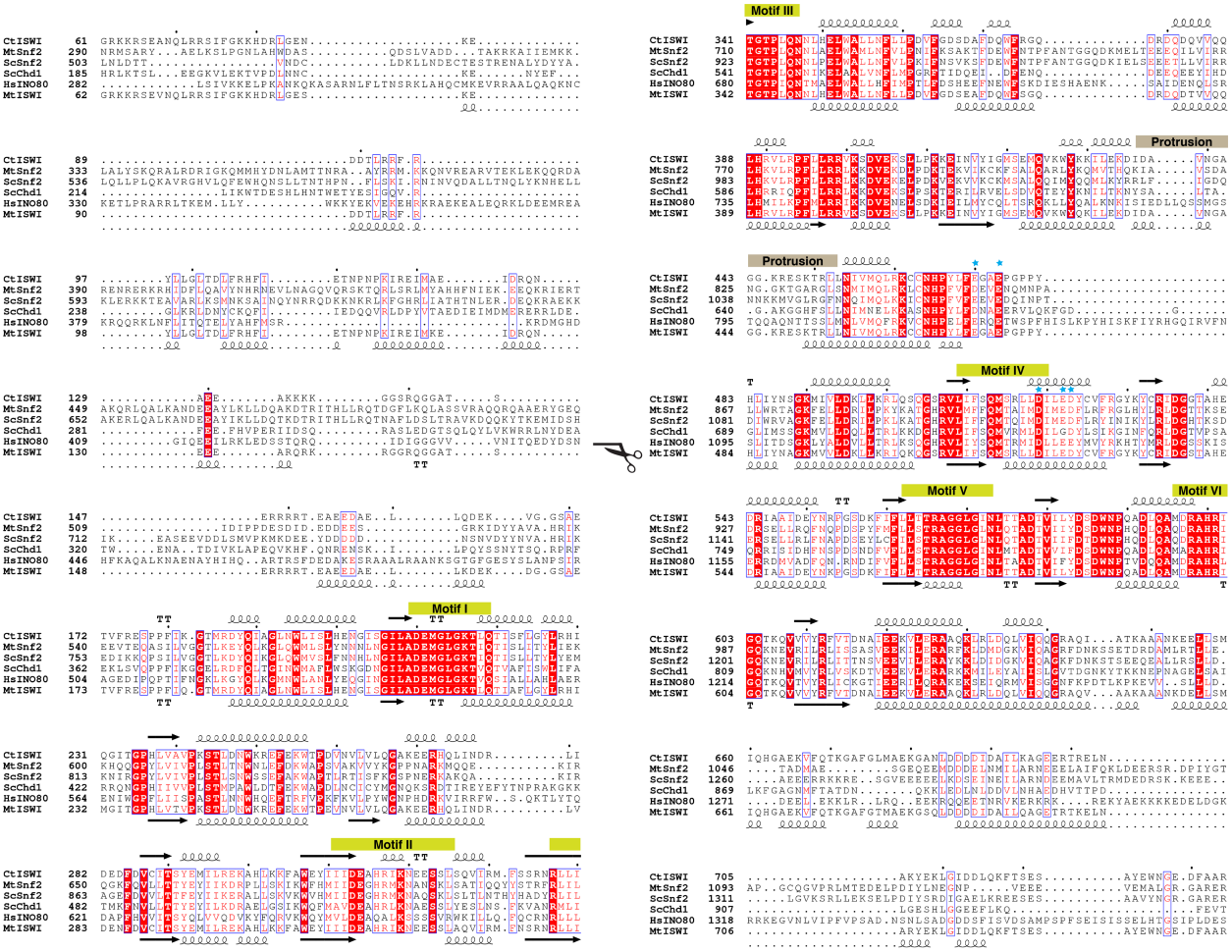

Figure S6. Sequence alignments of ISWI, SNF2, CHD1, and INO80 subfamily of remodelers. Secondary structural assignments on the top are based on the nucleosome bound CtISWI structure determined in this study while the bottom is based on the nucleosome free MtISWI structure (PDB 5JXR). Alignments corresponding to the N- and C-terminals as well as an intermediate region where the alignment is predominantly occupied by a large insertion in the HsINO80 (residues H855–E1034, indicated by scissors) are not shown for clarity. The helicase motifs are shown above the alignments. The acidic residues of CtISWI implicated in binding the basic N-tail of histone H4 are highlighted by blue star on the top. Strictly conserved residues

among all the remodelers included in the alignment are highlighted in white characters on red background.

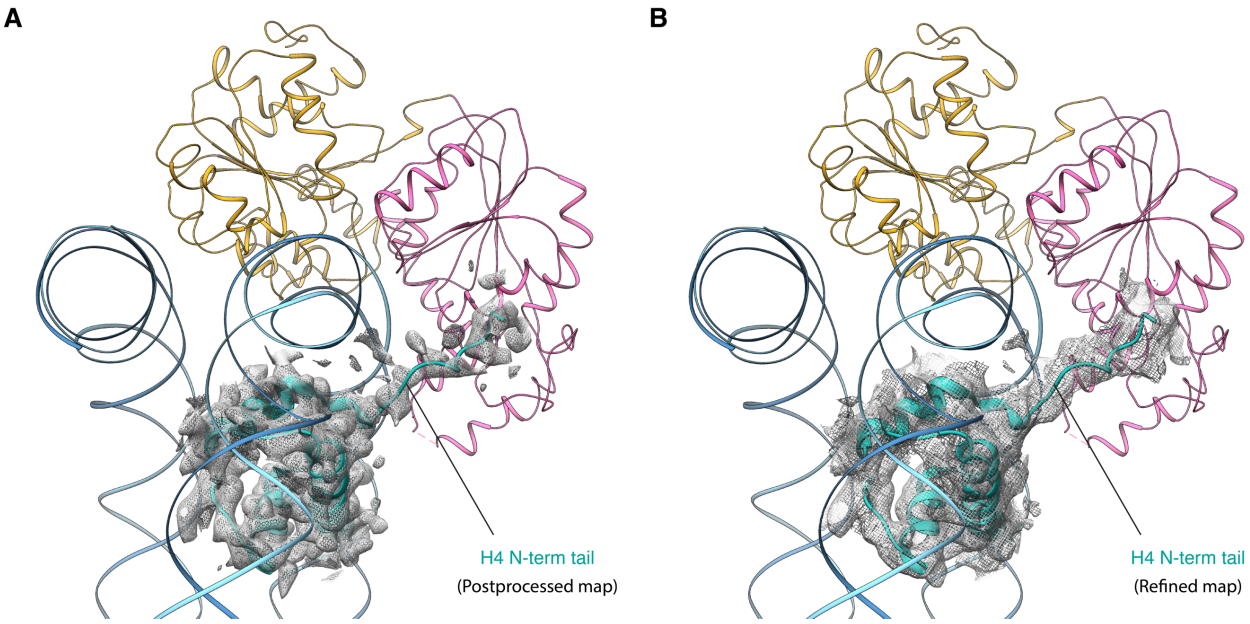

Figure S7. Binding between the N-terminal tail of histone H4 and CtISWI. (A and B) A view to illustrate the protrusion of the N-terminal tail of the H4 to bind the core 2 of the ATPase domain of ISWI. Density corresponding to the sharpened (A) and the refined (B) maps is also shown for the histone H4. The N-terminal tail of H4 is highly flexible and though it gets stabilized to an extent due to its interactions with the bound ISWI, the tail residues still show a high degree of disorder that results in the broken density upon B-factor sharpening. However, the refined map prior to the sharpening step allows for a better visualization of the path taken by the N-terminal tail of the H4.

Table S1. Cryo-EM data collection and structure determination statistics.

Data acquisition and image processing	**CtISWI$_{77\text{-}\Delta\text{-}722}$-nucleosome**
Grids	Quantifoil R 1.2/1.3, 200 mesh
Robot	Leica EM GP
Micrographs	1,948
Particles (Autopick)	570,527
Particles retained after 2D classification	480,472
Particles in final 3D reconstruction	32,529 (CtISWI$_{77\text{-}\Delta\text{-}722}$-nucleosome) 52,917 (Nucleosome)
Symmetry	C1
Map sharepening B-factor (Å^2)	-144 (CtISWI$_{77\text{-}\Delta\text{-}722}$-nucleosome) -141 (Nucleosome)
Resolution (Å)	4.07 (CtISWI$_{77\text{-}\Delta\text{-}722}$-nucleosome) 3.95 (Nucleosome)

Model building and structure refinement	**CtISWI$_{77\text{-}\Delta\text{-}722}$-nucleosome**	**Nucleosome**
Number of atoms	15197	11923
Geomtric parameters (r.m.s.d.)		
Bond length (Å)	0.009	0.010
Bond angle (°)	1.005	0.920
Ramachandran plot (%)		
Favored	90.24	92.31
Allowed	9.76	7.42
Outliers	0.00	0.27
Molprobity		
Overall score	1.88	1.76
Clash score	6.18	5.37
Rotamers outliers (%)	0.11	0.00
Cβ outliers (%)	0.00	0.00
Model-map correlation	0.76	0.80
EMRinger score	2.49	2.98